Differences in BVOC oxidation and SOA formation above and below the forest canopy

Benjamin C. Schulze[1], Henry W. Wallace[1], James H. Flynn[2], Barry L. Lefer[3], Matt H. Erickson[2], B. Thomas Jobson[4], Sebastien Dusanter[5,6,7], Stephen M. Griffith[7,‡], Robert F. Hansen[8,^], Philip S. Stevens[8], Robert J. Griffin[1*]

[1] Department of Civil and Environmental Engineering, Rice University, Houston, TX, 77004

[2] Department of Earth and Atmospheric Sciences, University of Houston, Houston, TX, 77204

[3] Airborne Sciences Program, NASA, Washington, DC, 20546

[4] Department of Civil and Environmental Engineering, Laboratory for Atmospheric Research, Washington State University, Pullman, WA, 99164

[5] Mines Douai, SAGE, F-59508 Douai, France

[6] Université de Lille, 59655 Villeneuve d'Ascq, France

[7] School of Public and Environmental Affairs, Indiana University, Bloomington, IN, USA

[8] Department of Chemistry, Indiana University, Bloomington, IN, USA

[‡] Now at Department of Chemistry, The Hong Kong University of Science and Technology, Kowloon, Hong Kong

[^] Now at School of Chemistry, University of Leeds, Leeds, UK LS2 9JT

[*] Corresponding author: 713-348-2093, rob.griffin@rice.edu

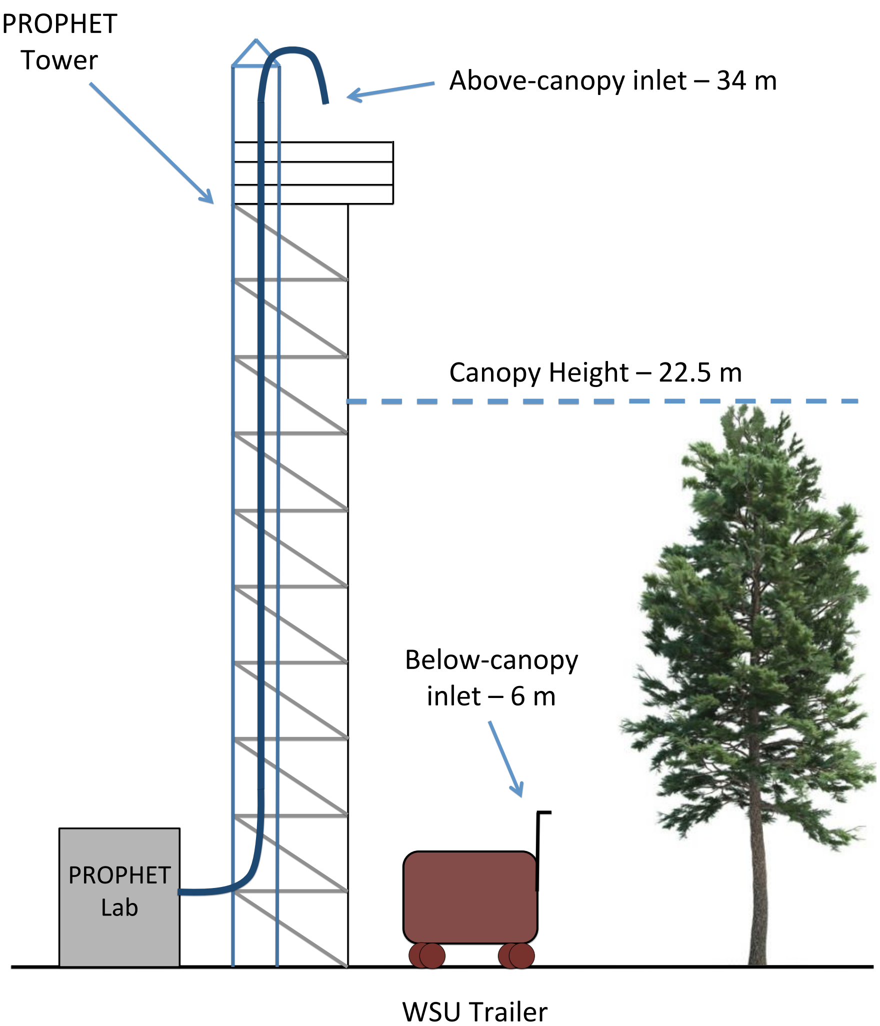

Figure S1. Depiction of the PROPHET tower and inlet locations used during CABINEX 2009.

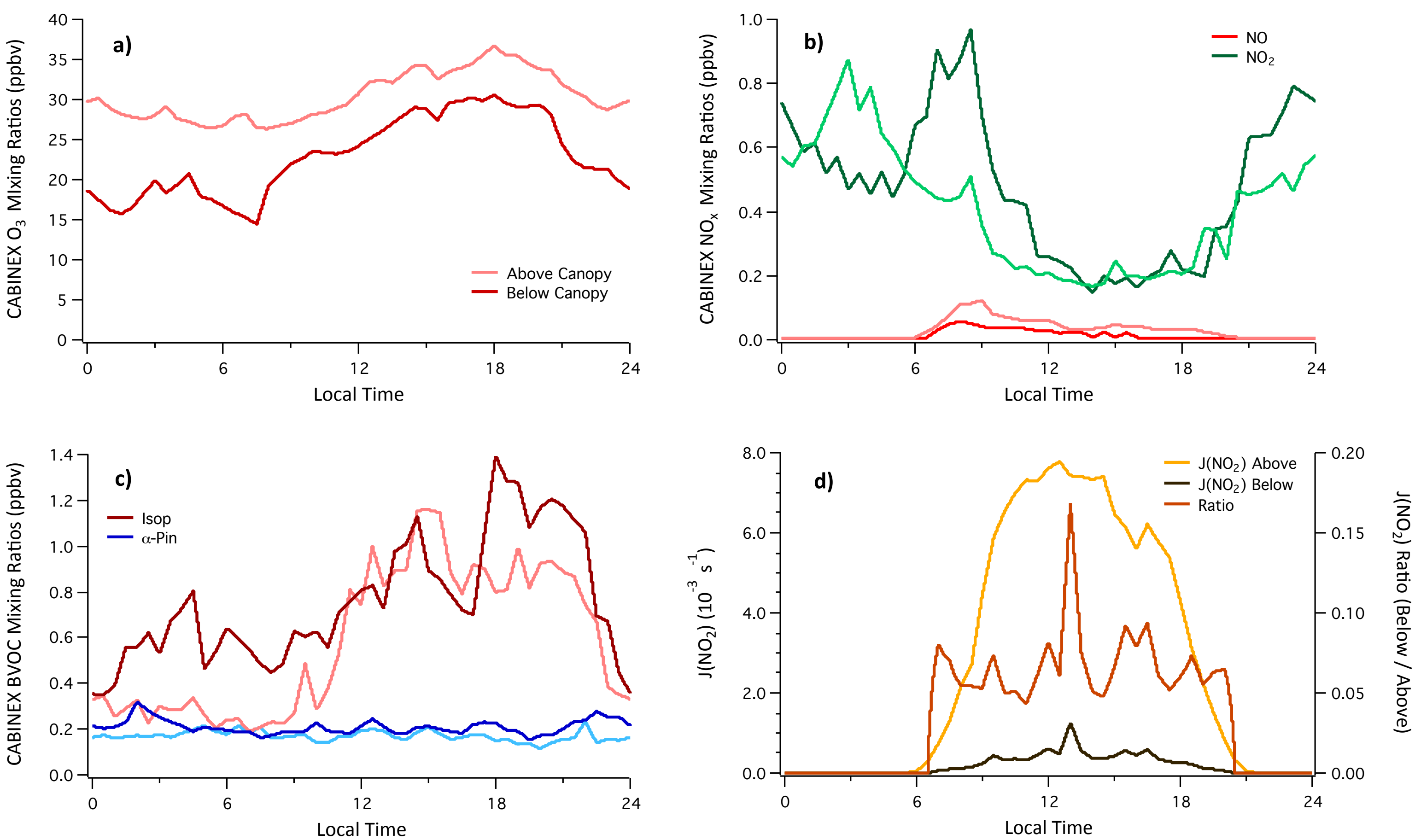

Figure S2. CABINEX 2009 median measurements of **(a)** ambient O_3 mixing ratios, **(b)** ambient NO_x mixing ratios, **(c)** ambient isoprene and α-pinene mixing ratios, and **(d)** the photolysis rate of NO_2.

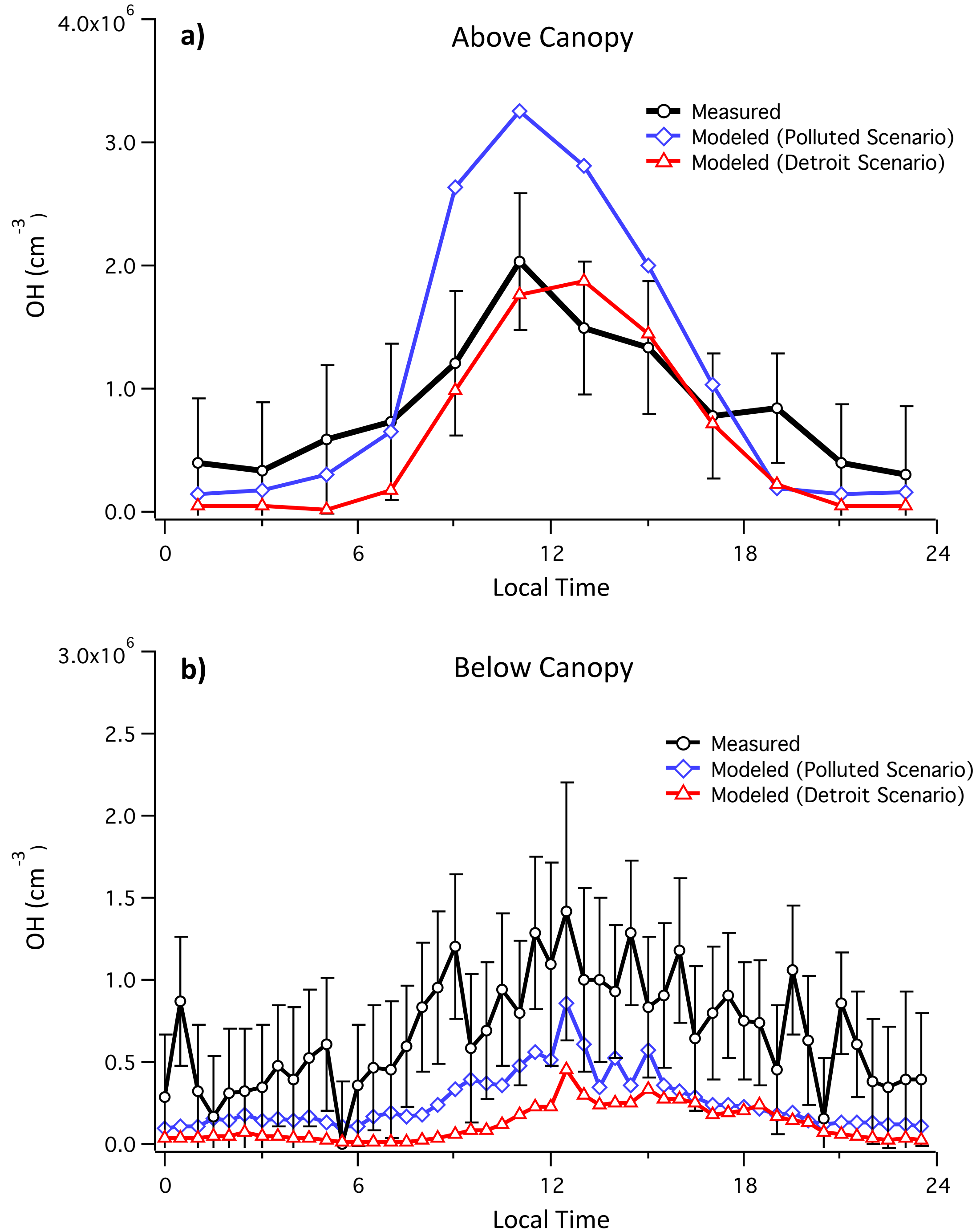

Figure S3. (a) Comparison of median above-canopy OH measurements during CABINEX 2009 to 0D model predictions for the artificially polluted and Detroit scenarios **(b)** Comparison of median below-canopy OH measurements during CABINEX 2009 to 0D model predictions for the artificially polluted and Detroit scenarios. Error bars indicate median measurement precision. Above-canopy OH measurements were averaged over 2 hour intervals, while below-canopy measurements were averaged over 30 minutes intervals.

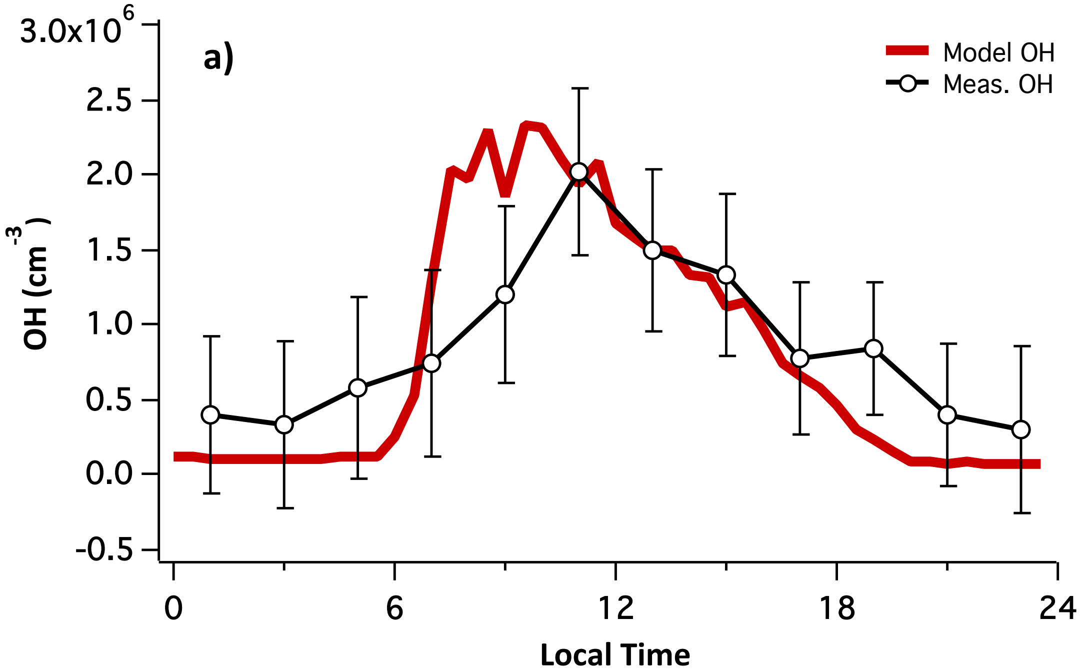

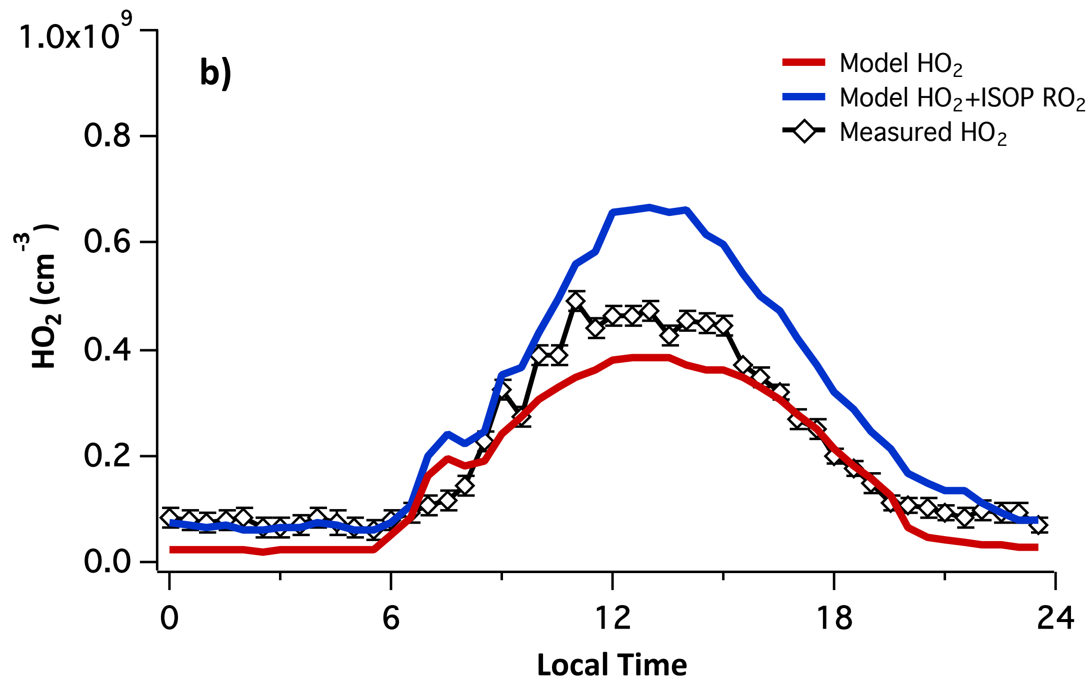

Figure S4. **(a)** Comparison of above-canopy median OH measurements during CABINEX 2009 to 0D model predictions for the ambient CABINEX model scenario. **(b)** Comparison of above-canopy median HO_2 measurements during CABINEX 2009 to 0D model predictions of HO_2 and HO_2 + isoprene RO_2 for the ambient CABINEX model scenario. Error bars indicate median measurement precision.

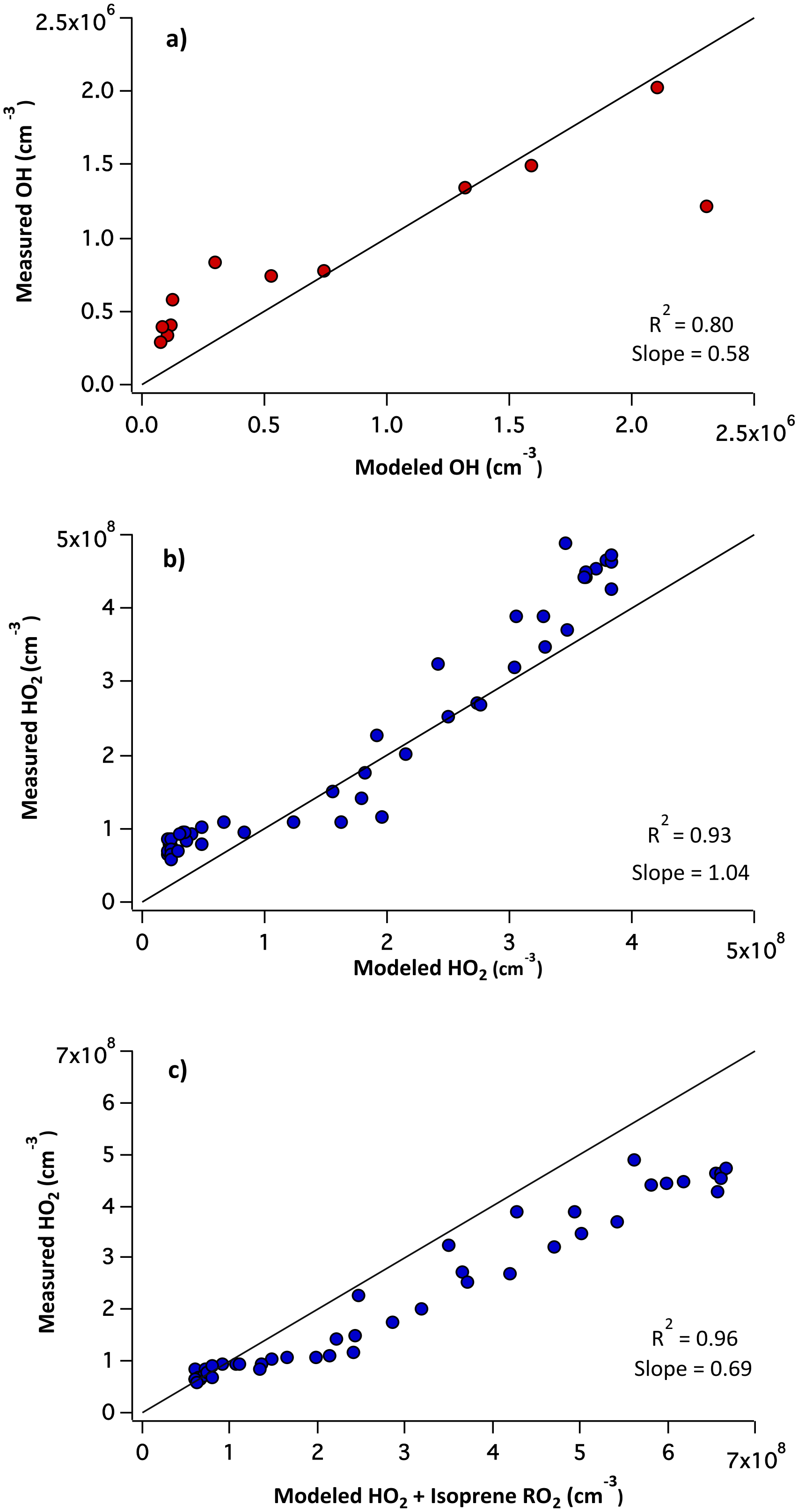

Figure S5. Linear regression of **(a)** median OH measurements during CABINEX 2009 and 0D model predictions, **(b)** median HO_2 measurements and 0D model predictions, and **(c)** median HO_2 measurements and HO_2 + isoprene RO_2 0D model predictions. The 1:1 line is included in each plot.

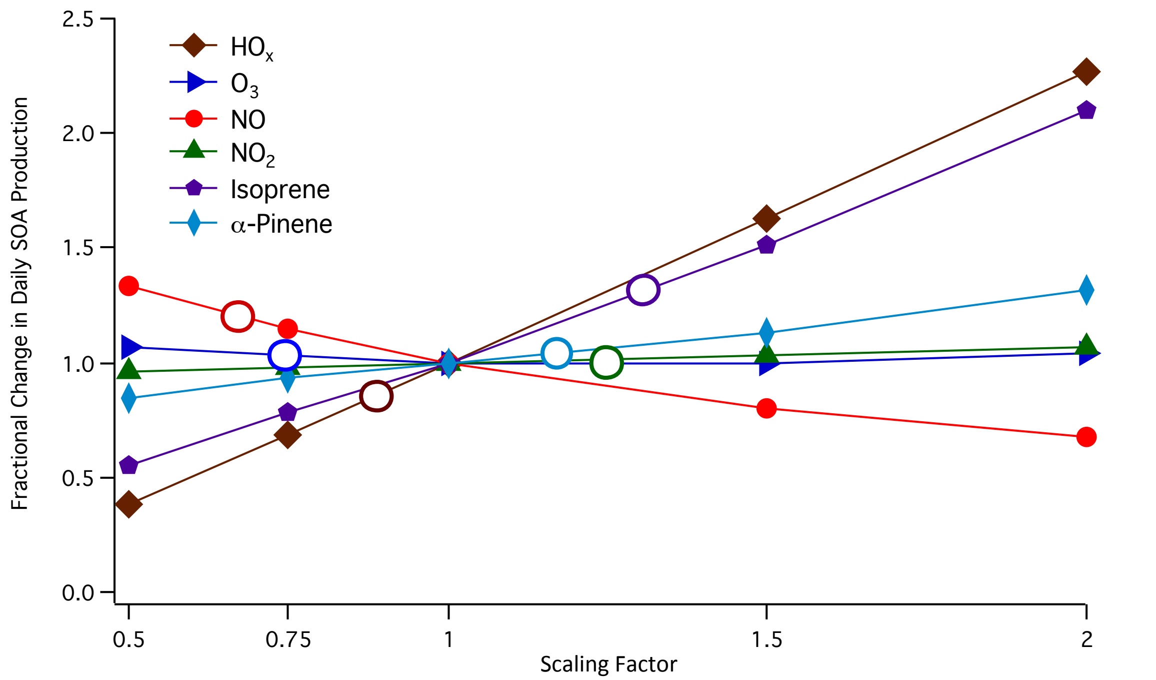

Figure S6. Sensitivity analysis of total daily SOA production in the above-canopy ambient scenario from scaled changes in NO, NO_2, O_3, HO_x, isoprene, and α-pinene. White circles indicate expected change below the canopy based on observed gradients in mixing ratios of these species. For instance, NO concentrations are on average 33% lower below the canopy than above (67% of above canopy concentrations), which, assuming concentration gradients of individual species affect SOA production independently, would result in approximately a 25% increase in total daily SOA production below the canopy relative to above. It is apparent that SOA production is most sensitive to NO, isoprene, and HO_x, and the below-canopy enhancement of SOA production is largely the result of the NO and isoprene gradients.

Table S1. Description of dominant $RONO_2$ oxidation products in α-pinene SOA as characterized by the Leeds Master Chemical Mechanism. Diurnal profiles of these species are plotted in Figure 10. Column 4 indicates the initial oxidant(s) that reacts with α-pinene to eventually produce the given species.

MCM Name	Chemical Structure	Chemical Formula	MW	Formation Pathway
NC102OOH	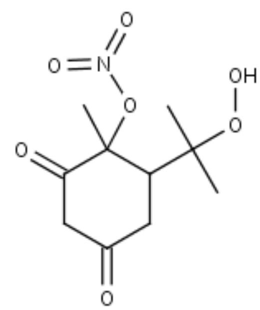	$C_{10}H_{15}NO_7$	261.2286	NO_3
NAPINAOOH	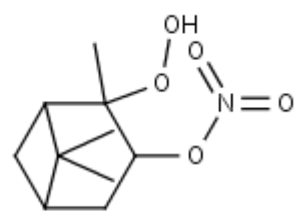	$C_{10}H_{17}NO_5$	231.2457	NO_3
NAPINBOOH	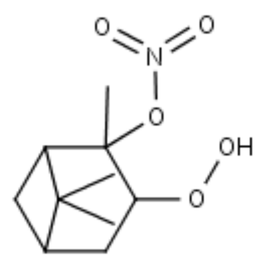	$C_{10}H_{17}NO_5$	231.2457	NO_3
NC101OOH	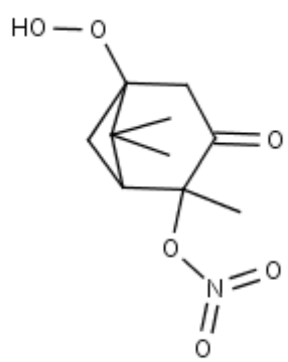	$C_{10}H_{15}NO_6$	245.2292	NO_3

NC71OOH	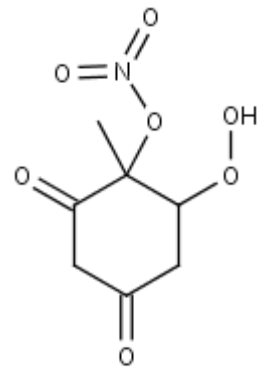	$C_7H_9NO_7$	219.1489	NO_3
NC6PAN1	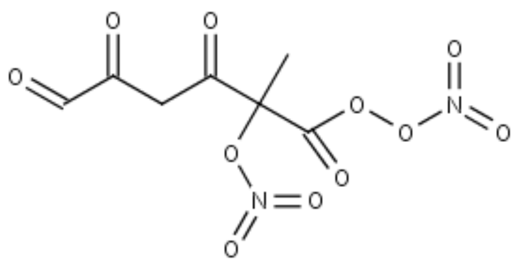	$C_7H_6N_2O_{11}$	294.1293	NO_3
C717NO3	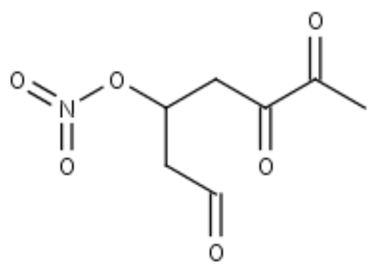	$C_7H_9NO_6$	203.1495	O_3
C108NO3	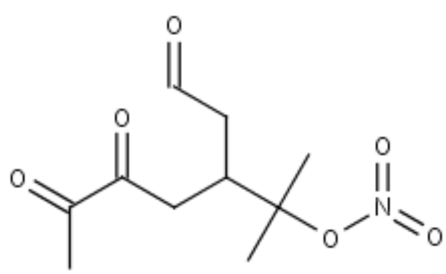	$C_{10}H_{15}NO_6$	245.2292	O_3
APINANO3	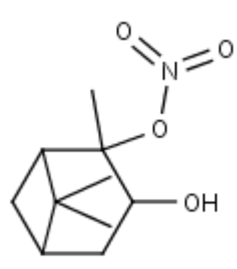	$C_{10}H_{17}NO_4$	215.2463	NO_3, OH

APINBNO3	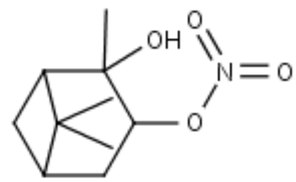	$C_{10}H_{17}NO_4$	215.2463	NO_3, OH
C98NO3	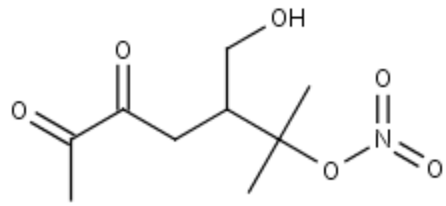	$C_9H_{15}NO_6$	233.2185	NO_3, O_3, OH
C106NO3	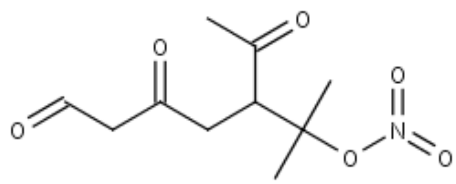	$C_{10}H_{15}NO_6$	245.2292	NO_3, O_3, OH
PINALNO3	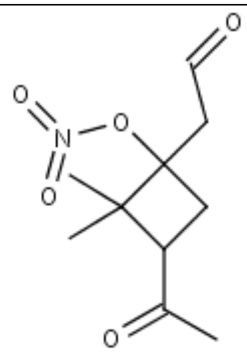	$C_{10}H_{15}NO_5$	229.2298	NO_3, O_3, OH

Table S2. Description of dominant $RONO_2$ oxidation products in isoprene SOA as characterized by the Leeds Master Chemical Mechanism. Diurnal profiles of these species are plotted in Figure 11. Column 4 indicates the initial oxidant(s) that reacts with isoprene to eventually produce the given species.

MCM Name	Chemical Structure	Chemical Formula	MW	Formation Pathway
C510OOH	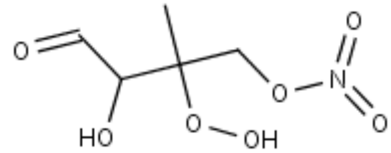	$C_5H_9NO_7$	195.1275	NO_3
INDOOH	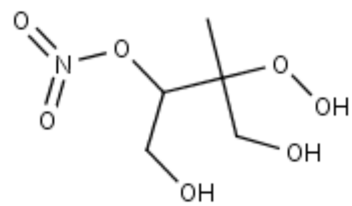	$C_5H_{11}NO_7$	197.1433	OH
NC524OOH	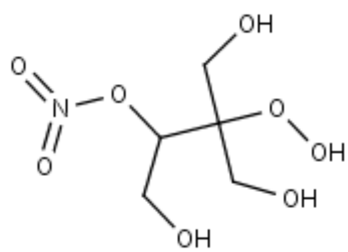	$C_5H_{11}NO_8$	213.1427	OH
INAOOH	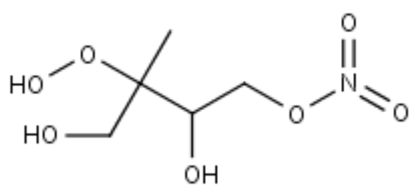	$C_5H_{11}NO_7$	197.1433	OH
INB1OOH	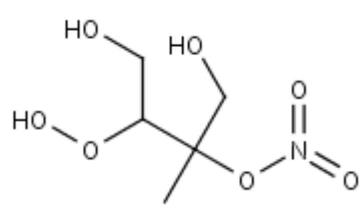	$C_5H_{11}NO_7$	197.1433	OH

NC524NO3	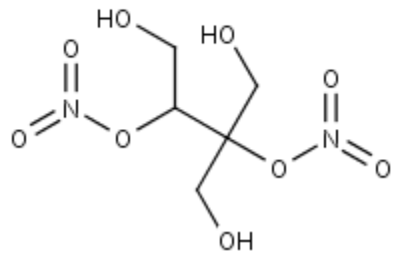	$C_5H_{10}N_2O_9$	242.1409	OH
INB1NO3	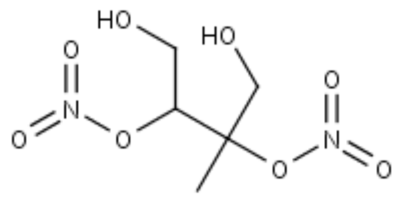	$C_5H_{10}N_2O_8$	226.1415	OH
INB2OOH	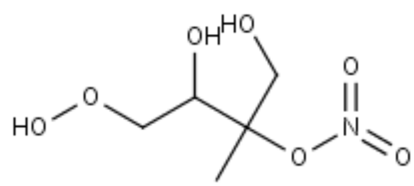	$C_5H_{11}NO_7$	197.1433	OH
INANO3	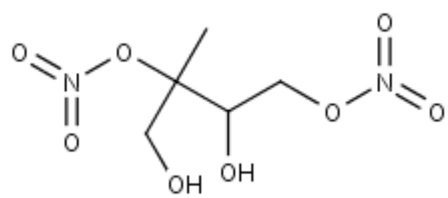	$C_5H_{10}N_2O_8$	226.1415	OH
INDHPPAN	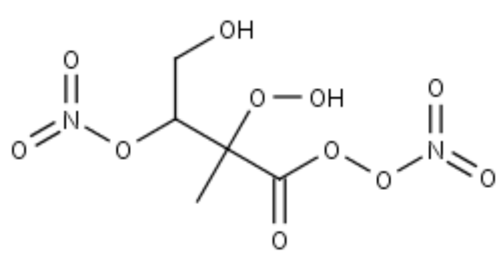	$C_5H_8N_2O_{11}$	272.1238	OH
C58NO3PAN	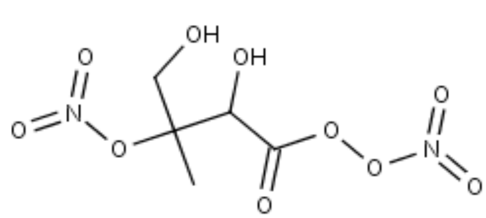	$C_5H_8N_2O_{10}$	256.1244	OH

INAHCO3	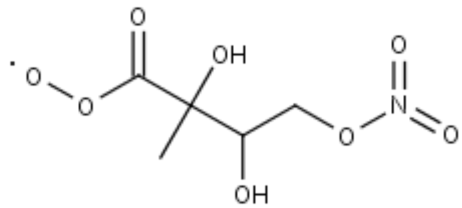	$C_5H_8NO_8$	210.1189	OH
INCOOH	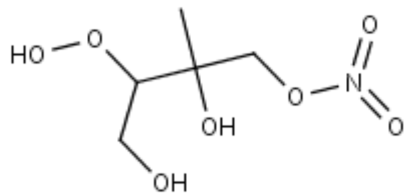	$C_5H_{11}NO_7$	197.1433	NO_3, OH
INCNO3	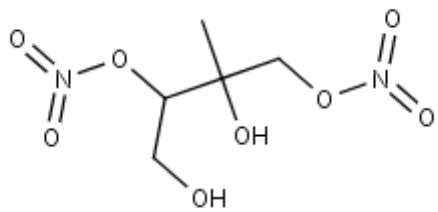	$C_5H_{10}N_2O_8$	226.1415	NO_3, OH